



Evaluation of 5-hydroxy-1,4-naphthoquinone-cobalt(III) complexes for hypoxia-activated drug delivery

Marcos Vinícius Palmeira de Mello^a, Gerardo Cebrián-Torrejón^a, Jonas Ramos Pereira^b, Caroline dos Santos Moreira^a, Carinne Borges de Souza Moraes Rego Gomes^a, David Rodrigues da Rocha^a, Elaine Maria de Souza Fagundes^b, Glaucio Braga Ferreira^a, Mauricio Lanznaster^{a,*}

^a Instituto de Química, Universidade Federal Fluminense, Outeiro S. João Batista S/N, 24020-141 Niterói, RJ, Brazil

^b Instituto de Ciências Biológicas, Universidade Federal de Minas Gerais, Av. Antônio Carlos 6627, 30123-970 Belo Horizonte, MG, Brazil

ABSTRACT

Three novel Py_2N_2 cobalt(III) complexes with the 5-hydroxy-1,4-naphthoquinone nuclei (NQ) were evaluated as potential hypoxia-activated anticancer prodrugs. The complexes were synthesized and fully characterized by IR and UV–Visible spectroscopies, ESI mass spectrometry and CHN elemental analysis. Structural information was obtained from density functional theory (DFT) calculations. Cyclic voltammetry analysis in acetonitrile indicates that the ligand substituents (H, CH_3 and *p*-tolylthio) do not have a relevant effect on the $\text{Co}^{3+}/\text{Co}^{2+}$ redox potential. Reactions with ascorbic acid in phosphate buffers were performed to simulate redox activation of the complexes in biological media. Fast and irreversible dissociation of the NQ ligands was observed for all complexes upon $\text{Co}^{3+}/\text{Co}^{2+}$ reduction. Cytotoxic activity of complexes **1** and **3** was evaluated in tumor cells (HT-29 and HCT-116) under hypoxic and normoxic conditions.

1. Introduction

Conventional anticancer treatments such as radiation and chemotherapy have limited efficacy in certain types of solid tumors, as a consequence of inefficient vascularization that generates areas of low O_2 concentrations, called hypoxic regions [1]. Nonetheless, differentiation of hypoxic tumor cells from the normoxic tissue provides a target that has been exploited for development of new therapeutic strategies [2]. Metal complexes with two biologically accessible oxidation states such as platinum, ruthenium and cobalt are of special interest. These metals are kinetically inert in their higher oxidation state (Pt^{4+} , Ru^{3+} and Co^{3+}), but become labile when reduced [3]. Reduction in hypoxic tissues is facilitated due to the lower concentration of O_2 and consequent higher concentration of biological reducing agents [4,5]. Thus, prodrug candidates based on such metals have been designed to circulate intact through the organism in their inert form. When the hypoxic tissues of a tumor are reached, the prodrug is activated by reduction to its labile form, facilitating ligand exchange reactions [3,6]. For platinum and ruthenium, the metal is usually responsible for the cytotoxic activity by binding biologically relevant targets such as DNA [3]. Cobalt, on the other hand, functions as a carrier of drugs that are deactivated upon coordination to the metal ion in its inert +3 oxidation state [6]. Selective redox activation to Co^{2+} under hypoxic conditions triggers the dissociation of the drug in its

active form. If reduction takes place in normoxic tissue, oxidation back to Co^{3+} by O_2 should prevent dissociation of the drug [7,8]. A number of cobalt complexes have already been investigated, with promising results [6,8–11]. Some key selected examples are those with nitrogen mustards and 8-hydroxyquinolines, described by Ware and coworkers [12–19], and with hydroxamic acids and curcumin, described by Hambley and coworkers [20–23] (Fig. 1). Despite all affords so far none presented the necessary requirements to reach clinical trials. To achieve this goal, our group has focused on the investigation of the kinetic and thermodynamic parameters associated with the reactivity of cobalt prodrugs (inertia of the Co^{3+} species, lability and stability of the Co^{2+} complex, kinetics of ligand dissociation, redox potential, etc.). In this way, we have been studying a series of cobalt(III) complexes containing the naphthoquinone nuclei (NQ) as potential candidates for hypoxia-selective redox-activated drug delivery [24–28]. In a previous work, the complex $[\text{Co}^{\text{III}}(\text{bhnq})(\text{py}_2\text{en})]^+$ was obtained from the reaction of lawsone (2-hydroxy-1,4-naphthoquinone) with a cobalt(II) salt and the ancillary ligand *N,N'*-bis(pyridin-2-ylmethyl)ethylenediamine, py_2en [24,27]. Dimerization of lawsone took place *in situ* to generate bis-(2-hydroxy-1,4-naphthoquinonate), bhnq^{2-} . The redox potential of the complex (-0.22 V vs. SHE) was within the accepted ideal range (-0.2 to -0.4 V vs. SHE) for redox activation in biological conditions and an O_2 -dependent dissociation of bhnq^{2-} from the complex upon reduction was observed. Interestingly, methylation of the ancillary ligand py_2en

* Corresponding author.

E-mail address: ml@id.uff.br (M. Lanznaster).

<https://doi.org/10.1016/j.jinorgbio.2019.110756>

Received 19 March 2019; Received in revised form 23 June 2019; Accepted 24 June 2019

Available online 25 June 2019

0162-0134/ © 2019 Elsevier Inc. All rights reserved.

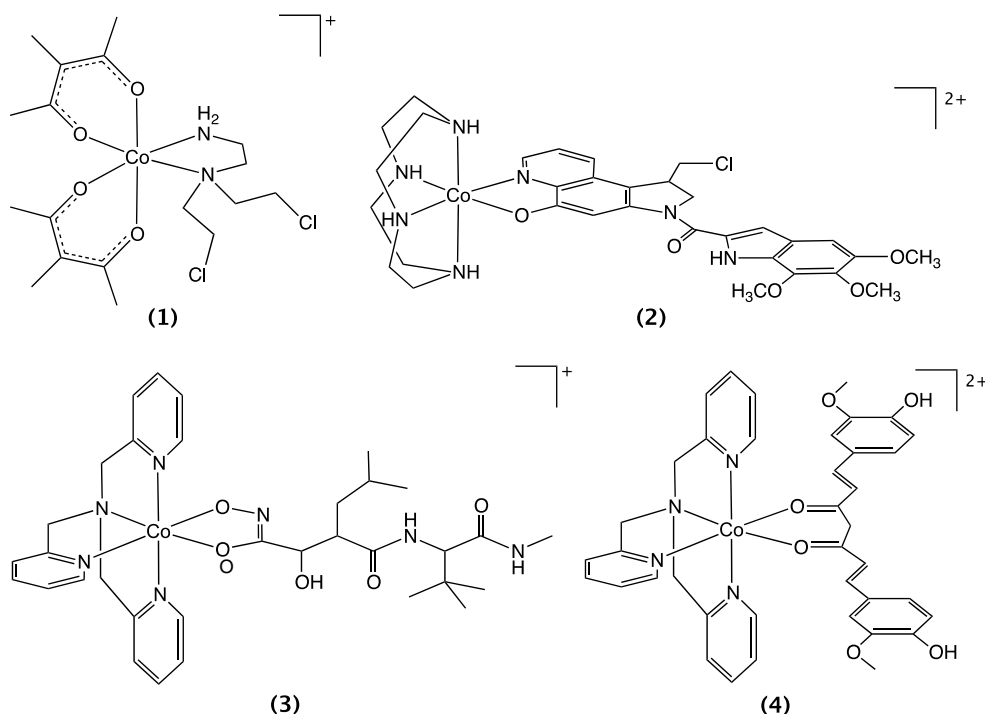


Fig. 1. Examples of relevant cobalt(III) complexes investigated as prodrugs for hypoxia activated drug delivery: (1) $[\text{Co}(\text{Meaac})_2(\text{DCE})]^+$ [12–14], (2) $[\text{Co}(\text{cyclen})(\text{azaCBI})]^{2+}$ [18], (3) $[\text{Co}(\text{mmst})(\text{tpa})]^+$ [20], (4) $[\text{Co}(\text{curcumin})(\text{tpa})]^{2+}$ [21–23].

changed the $\text{Co}^{3+}/\text{Co}^{2+}$ potential (-0.08 V vs. SHE); thus ligand dissociation became O_2 -independent [24,27]. More recently, a series of cobalt(III) complexes $[\text{Co}(\text{NQ-X})(\text{TPA})]^{2+}$ (TPA = tris(2-pyridylmethyl)amine) was investigated, with lawsone derivatives (NQ-X) containing substituents at the 3-position of aromatic ring ($X = \text{CH}_3, \text{Cl}, \text{Br}, \text{I}$) [28]. Dimerization to form bhnq^{2+} was hampered, but the coordinated NQ-X derivatives with electron withdrawing substituents ($X = \text{Cl}, \text{Br}$ and I) activated the carbonyl-C1 carbon atom for a nucleophilic attack of the solvent (methanol). The redox potential for these complexes shifted away ($+0.21/+0.33\text{ V vs. SHE}$) from the accepted ideal range [28]. Simulations of redox activation by ascorbic acid revealed a lack of hypoxic selectivity, with a fast O_2 -independent dissociation of NQ-X upon reduction. In both situations, neither of the naphthoquinones (bhnq and NQ-X) were cytotoxic, thus preventing additional evaluation of biological activity. In a continuation of our effort to investigate cobalt(III)-naphthoquinone systems as potential candidates for anticancer prodrugs, we describe here three novel cobalt(III) complexes, $[\text{Co}^{\text{III}}(\text{NQ1})(\text{py}_2\text{en})(\text{ClO}_4)_2 \cdot 2\text{H}_2\text{O}$ (1), $[\text{Co}^{\text{III}}(\text{NQ2})(\text{py}_2\text{en})(\text{ClO}_4)_2 \cdot 4\text{H}_2\text{O}$ (2) and $[\text{Co}^{\text{III}}(\text{NQ3})(\text{py}_2\text{en})(\text{ClO}_4)_2 \cdot 2\text{H}_2\text{O}$ (3), where py_2en is the ancillary ligand N,N' -bis(pyridine-2-ylmethyl)ethylenediamine, NQ1 is 5-hydroxy-1,4-naphthoquinone (Juglone), NQ2 is 5-hydroxy-2-(*p*-tolylthio)-1,4-naphthoquinone and NQ3 is 5-hydroxy-2-methyl-1,4-naphthoquinone (Plumbagin) (Fig. 2). Juglone, plumbagin and their derivatives are known for a broad spectrum of biological

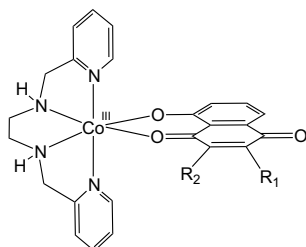


Fig. 2. Complexes of general formula $[\text{Co}^{\text{III}}(\text{NQ})(\text{py}_2\text{en})]^{2+}$: (1), $R_1 = R_2 = \text{H}$ (NQ1); (2), $R_1 = \text{H}, R_2 = \text{SC}_6\text{H}_4\text{CH}_3$ (NQ2); (3) $R_1 = \text{CH}_3, R_2 = \text{H}$ (NQ3).

activities, including antitumor properties [29–36], thus allowing the use of biological assays to further evaluate their cobalt(III) complexes as prodrug candidates against cancer cells. Hence, the present work focuses on investigating the properties and reactivity of cobalt(III) complexes with juglone and its derivatives, as well as their activity against cancer cells under hypoxia and normoxia.

2. Experimental

2.1. Material and instruments details

All starting materials, including juglone and plumbagin (Sigma-Aldrich), were purchased from commercial sources and used without further purification. Infrared spectra were measured in a Varian 600 FTIR equipped with a Pike ATR Miracle accessory (diamond/ZnSe crystal, resolution: 4 cm^{-1}). UV-Visible spectra were collected from solutions in spectroscopic grade solvents, using a Varian Cary 50 spectrophotometer. Microanalyses were performed in a Perkin-Elmer CHN 2400 micro analyzer at Universidade de São Paulo (USP-SP), Brazil. Electron spray ionization mass spectrometry (ESI-MS) spectra were obtained by direct infusion in a Perkin Elmer SQ-300 mass spectrometer, using acetonitrile or methanol (MS grade) as solvent, at CAPEX 50. Electrochemical experiments were performed in acetonitrile (HPLC grade) in a BASi Epsilon Potenciostat-Galvanostat at room temperature under argon atmosphere, using 0.10 M of tetrabutylammonium perchlorate (TBAClO_4) as supporting electrolyte. A standard three-component system was used: a glassy carbon working electrode, a platinum wire auxiliary electrode, and an Ag/AgCl reference electrode. Ferrocene (Fc/Fc^+) ($E^\circ = 0.4\text{ V vs SHE}$) was used as internal reference [37,38].

2.2. Syntheses

The ligands N,N' -bis(pyridin-2-ylmethyl)ethylenediamine (py_2en) and 5-hydroxy-2-(*p*-tolylthio)-1,4-naphthoquinone (NQ2) were prepared following procedures described elsewhere [39–41].

Caution: Although the authors did not have problems, perchlorate salts of metal complexes are potentially explosive and should be handled with care only in small quantities.

[Co(NO₂)₂(py₂en)]ClO₄·0.5H₂O was prepared by following previously reported procedures [42,43]. To a solution of Na₃[Co(NO₂)₆] (2.0 mmol) in 10 mL of water was added an aqueous solution (10 mL) of py₂en (2.0 mmol). After stirring the mixture for 1 h, LiClO₄ was added (10 mmol). The mixture was stirred for another hour and cooled in an ice bath. The product precipitated as a yellow powder, which was filtered out, washed with diethyl ether and dried under vacuum. Yield: 44%. IR (ATR, cm⁻¹): 1610, 1443 (C=C, C=N); 1408, 1345 (O – N=O); 1093 (Cl – O). Anal. calc. for C₁₄H₁₉ClCoN₆O_{8.5}: C, 33.52; H, 3.82; N, 16.75%. Found: C, 33.64; H, 3.81; N, 16.71%. ESI-MS (MeOH): m/z⁺ = 393.09, 100% for [Co(NO₂)₂(py₂en)]⁺.

[Co(OSO₂CF₃)₂(py₂en)]CF₃SO₃ was obtained by the reaction of [Co(NO₂)₂(py₂en)]ClO₄·0.5H₂O (1 mmol) with triflic acid (5 mL) at 40 °C under argon atmosphere and magnetic stirring for 30 min. Then, the reaction solution was cooled to 0 °C in ice bath and diethyl ether was added dropwise up to the precipitation of the product. A pink solid was isolated by vacuum filtration inside of a glove bag filled with argon, washed with diethyl ether, and storage in a – 30 °C freezer. Yield: 65%. IR (ATR, 4000–600 cm⁻¹): 3263 (N – H); 1612, 1444 (C=C, C=N); 1214, 1005 (O – S=O); 1168, 1031 (C – F).

General procedure for the synthesis of 1–3. A methanol solution (10 mL) of the NQ (0.3 mmol) and Et₃N (0.3 mmol) was added to a methanol solution (10 mL) of [Co(OSO₂CF₃)₂(py₂en)]CF₃SO₃ (0.3 mmol). Then, LiClO₄ (1.5 mmol) was added and the reaction was kept under magnetic stirring at room temperature. After 4 h, the reaction solution was filtered and diethyl ether was added dropwise until the formation of a violet precipitate. The product was isolated by vacuum filtration, washed with diethyl ether and dried under vacuum.

2.2.1. [Co(NQ1)(py₂en)](ClO₄)₂·2H₂O (1)

Yield. 45%. IR (ATR, 4000–600 cm⁻¹): 3194 (N – H); 1510, 1423 (C=C, C=N); 1622, 1591 (C=O); 1290 (C – O); 1095 (Cl – O). Anal. Calc. for C₂₄H₂₇Cl₂CoN₄O₁₃: C, 40.64; H, 3.84; N, 7.90%. Found: C, 40.82; H, 3.97; N, 7.71%. ESI-MS (MeCN): m/z²⁺ = 236.9, 100% for [Co(NQ1)(py₂en)]²⁺.

2.2.2. [Co(NQ2)(py₂en)](ClO₄)₂·4H₂O (2)

Yield. 46%. IR (ATR, 4000–600 cm⁻¹): 3300 (N – H); 1506, 1417 (C=C, C=N); 1595, 1554 (C=O); 1244 (C – O); 1084 (Cl – O). Anal. Calc. for C₃₁H₃₇Cl₂CoN₄O₁₅: C, 42.92; H, 4.30; N, 6.46%. Found: C, 42.72; H, 4.03; N, 6.83%. ESI-MS (MeCN): m/z²⁺ = 297.9, 100% for [Co(NQ2)(py₂en)]²⁺.

2.2.3. [Co(NQ3)(py₂en)](ClO₄)₂·2H₂O (3)

Yield. 55%. IR (ATR, 4000–600 cm⁻¹): 3195 (N – H); 1510, 1421 (C=C, C=N); 1633, 1593 (C=O); 1252 (C – O); 1092 (Cl – O). Anal. Calc. for C₂₅H₂₉Cl₂CoN₄O₁₃: C, 41.51; H, 4.04; N, 7.75%. Found: C, 41.47; H, 4.00; N, 7.91%. ESI-MS (MeCN): m/z²⁺ = 243.8, 100% for [Co(NQ3)(py₂en)]²⁺.

2.3. Theoretical calculations

Theoretical calculations were carried out for the cations *cis*-α-[Co(NQ1)(py₂en)]²⁺ and *cis*-β-[Co(NQ1)(py₂en)]²⁺ considering them as non-interacting independent units. All calculations have been optimized from several initial geometries, in order to guarantee global minima energy structures. After this procedure, the vibrational calculations were performed. No imaginary modes were observed. In all calculations, the density functional theory method (DFT-PBE1PBE) with double zeta 6-311G** basis sets were used in the Gaussian 09 program [44]. Validation of the results was performed through single-point calculations with M06L, CAM-B3LYP, WB97XD and PBE1PBE-D3 methods that incorporate long-range corrected and dispersion effects. In

addition, the MP2 perturbative method was employed since this post-Hartree-Fock method recovers the electron correlation energy and serves as a reference result for the data obtained by DFT (see Table S1). All results were visualized using the graphical Chemcraft program [45,46].

2.4. Reactivity assays

The reactivity of complexes 1–3 towards ligand dissociation was evaluated in 0.05 M phosphate buffer solutions at pH 6.2, 7.0 and 7.4, prior and after reduction with ascorbic acid. Fresh stock solutions of the complexes (2.0 × 10⁻³ M) were prepared using HPLC grade DMSO. Stock solutions of phosphate buffer (0.05 M) were prepared by dissolving Na₂HPO₄ and NaH₂PO₄ in distilled water. The pH was adjusted to 6.2, 7.0 and 7.4 with NaOH 3.0 M. For the stability experiments, aliquots of 300 μL from the stock solutions of the complexes were diluted in 2700 μL of each phosphate buffer solution (pH 6.2, 7.0 and 7.4) in a 1 cm quartz cuvette, in order to obtain a final concentration of 2.0 × 10⁻⁴ M for the complexes. For the reduction experiments, fresh stock solutions (0.1 M) of ascorbic acid were prepared using distilled water. Aliquots of 150 μL from the stock solutions of the complexes and 100 μL from the stock solution of ascorbic acid were diluted in 150 μL of DMSO and added to 2600 μL of the buffer solutions, in 1 cm quartz cuvettes, in order to obtain final concentrations of 1.0 × 10⁻⁴ M and 1.0 × 10⁻³ M, respectively. For all experiments, the solutions were monitored over 72 h (1 h interval) at room temperature (25 ± 2 °C) in a Varian Cary 50 spectrophotometer with an 18-multicell accessory.

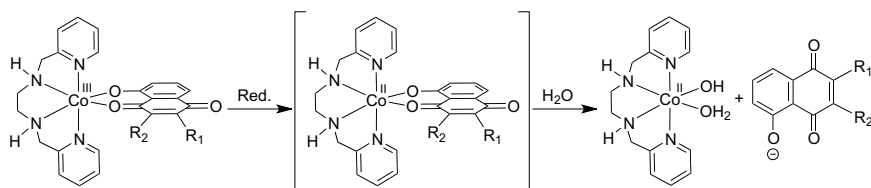
2.5. Cytotoxic activity

Colorectal adenocarcinoma (HT-29) and colorectal carcinoma (HCT-116) cells were kindly donated by Dr. Marcel Leist, University of Konstanz/Germany and maintained in Dulbecco's Modified Eagle Medium (DMEM, from Sigma Aldrich) with 10% fetal serum (GIBCO BRL, Grand Island, NY) and enriched with 1% antibiotic solution (100 IU/mL penicillin and 100 μg/mL streptomycin (GIBCO BRL, Grand Island, NY)). Cytotoxic activity was based on the mitochondrial reduction rate of 3-(4,5-dimethylthiazol-2-yl)-2,5-diphenyltetrazolium bromide (MTT) to formazan crystals [47]. Briefly, HT-29 and HCT-116 cells were plated at the density of 1 × 10⁴ cells per well (96-well plate). The cells were allowed to adhere overnight under hypoxic conditions (1% O₂, 5% CO₂, 94% N₂ at 37 °C) and normoxia (5% CO₂, 95% atmospheric air at 37 °C) as described by Harrison and coworkers [48]. After stabilization, all cells were incubated with the complexes 1–3 and the positive control Tirapazamine (TPZ) for 72 h, using seven serial 1:2 dilutions (100–1.56 μM), under conditions of hypoxia and normoxia. The IC₅₀ was calculated by non-linear regression using GraphPad Prism® Version 5.01 software (GraphPad Software Inc., La Jolla, CA, USA). All compounds were tested in three independent experiments performed in triplicate. DMSO (0.5%) was used as the control. The results were expressed as percentage of viability in relation to the negative control (DMSO, 0.5%), calculated as follows: percentage of cell viability (%) = [(OD of treated mean/OD negative control) × 100].

3. Results and discussions

3.1. Synthesis of complexes

The complexes [Co(NQ1)(py₂en)](ClO₄)₂·2H₂O (1), [Co(NQ2)(py₂en)](ClO₄)₂·4H₂O (2) and [Co(NQ3)(py₂en)](ClO₄)₂·2H₂O (3) were synthesized according with Scheme 1. The precursor complex [Co(NO₂)₂(py₂en)]ClO₄·0.5H₂O was obtained in the first step from the reaction between the ligand py₂en and Na₃[Co(NO₂)₆]·6H₂O, following a previously described procedure [42,43]. In the second step, [Co(NO₂)₂(py₂en)]ClO₄·0.5H₂O was treated with triflic acid under argon atmosphere, to produce the complex [Co(OSO₂CF₃)₂(py₂en)]CF₃SO₃



Scheme 1. Synthesis of complexes $[\text{Co}(\text{NQ})(\text{py}_2\text{en})]\text{ClO}_4 \cdot \text{XH}_2\text{O}$ (1–3): (i) water, 80 °C, 1 h, LiClO_4 ; (ii) triflic acid under argon atmosphere, 40 °C, 30 min; (iii) NQ, $\text{Et}_3\text{N}/\text{MeOH}$, room temperature, 4 h. (1) $\text{R}_1 = \text{R}_2 = \text{H}$; (2) $\text{R}_1 = \text{H}$, $\text{R}_2 = \text{SC}_6\text{H}_4\text{CH}_3$; (3) $\text{R}_1 = \text{CH}_3$, $\text{R}_2 = \text{H}$; $\text{OTf}^- = \text{O}_3\text{SCF}_3^-$.

[49]. Finally, complexes 1–3 were obtained from reactions between the precursor $[\text{Co}(\text{OSO}_2\text{CF}_3)_2(\text{py}_2\text{en})]\text{CF}_3\text{SO}_3$ and the naphthoquinones NQ1, NQ2 or NQ3, respectively, in methanol, at room temperature. Triethylamine was added as a base to deprotonate the naphthoquinones, and lithium perchlorate was added to guarantee an excess of the counterion to favor product precipitation. Repeated attempts to obtain X-ray suitable single crystals have been unsuccessful.

3.2. Spectroscopic and ESI-MS characterization

The IR spectra of complex $[\text{Co}(\text{NO}_2)_2(\text{py}_2\text{en})]\text{ClO}_4 \cdot 0.5\text{H}_2\text{O}$ (Fig. S1) present bands in 1408 and 1345 cm^{-1} assigned to the NO_2^- ligands and a band at 1093 cm^{-1} characteristic of the ClO_4^- counter-ion. For the precursor $[\text{Co}(\text{OSO}_2\text{CF}_3)_2(\text{py}_2\text{en})]\text{CF}_3\text{SO}_3$, bands assigned to the trifluoromethanesulfonate anion (OTf^-) were observed in the region of 1213–1001 cm^{-1} (Fig. S2). The IR spectra of complexes 1–3 (Figs. S3–S5) reveal the presence of intense bands in the region of 1506–1623 cm^{-1} , typical of C=O and C=C bonds of the naphthoquinone ligands [50–53]. The presence of ClO_4^- was also confirmed by intense bands in the region of 1095–1084 cm^{-1} [54]. Electrospray ionization mass spectrometry (ESI-MS) spectra of 1–3 in acetonitrile solutions show the peaks for the molecular ions of $[\text{Co}(\text{NQ1})(\text{py}_2\text{en})]^{2+}$, $[\text{Co}(\text{NQ2})(\text{py}_2\text{en})]^{2+}$ and $[\text{Co}(\text{NQ3})(\text{py}_2\text{en})]^{2+}$ as the main species in solution at, respectively, (m/z^{2+}) 236.9, 297.9 and 243.8 (Fig. S7). The UV–Vis spectra of complexes 1–3 and free naphthoquinone ligands (NQ1, NQ2 and NQ3) were recorded in acetonitrile (1.0×10^{-4} M) in the range of 200–800 nm (Fig. S8–S10). The spectrum of complex 1 (Fig. S11) shows two well-defined absorptions at 550 nm ($3.5 \times 10^3 \text{ M}^{-1} \text{ cm}^{-1}$) and 355 nm ($2.0 \times 10^3 \text{ M}^{-1} \text{ cm}^{-1}$). The low energy absorption is slightly shifted (bathochromically) in the spectrum of 2 (552 nm, $4.0 \times 10^3 \text{ M}^{-1} \text{ cm}^{-1}$, Fig. S12) and hypsochromically shifted in the spectrum of 3 (540 nm, $4.0 \times 10^3 \text{ M}^{-1} \text{ cm}^{-1}$, Fig. S13), respectively. Instead, the high-energy band in 3 has the same absorption maxima as complex 1 (355 nm, $3.5 \times 10^3 \text{ M}^{-1} \text{ cm}^{-1}$), while in complex 2 a shoulder is found at ~ 350 nm. The *p*-tolylthio in NQ2 seems to play a much stronger influence on the high-energy region of the spectrum of 2, while the effect of the methyl group in NQ3 is limited to the lower energy absorption in 3. These spectral features are similar to those observed for other complexes containing a naphthoquinone ligand and have been attributed to an overlapping of LMCT from the naphthoquinone skeleton to the cobalt(III) ion and naphthoquinone intra-ligand transitions [24,28,50]. The spectra of the free ligands NQ1 and NQ3 also present two absorptions in the regions of ~ 250 nm and ~ 410 nm, while a shoulder in ~ 290 nm and a band in ~ 410 nm is observed for NQ2.

3.3. Theoretical calculations

As single crystals suitable for X-ray could not be obtained for any of the complexes, structural analysis was carried out using DFT calculations. It has been observed that py_2en and similar tetradentate ligands with reduced amine linkage can wrap around a single metal center in different modes [53,55,56]. Thus, geometry optimizations were performed for the *cis*- α and *cis*- β isomers of $[\text{Co}(\text{NQ1})(\text{py}_2\text{en})]^{2+}$ (Fig. 3), employing the PBE1PBE hybrid functional [46]. Validation of the results was performed through single-point calculations with M06L, CAM-B3LYP, WB97XD, PBE1PBE-D3 and MP2 methods that

incorporate long-range corrected and dispersion effects (see Table S1). According to the variation of the total electronic energy (E^0) of the isomers, the *cis*- α is the most stable configuration adopted by complex 1 (Fig. 3). In this conformation, the two pyridine groups are coordinated *trans* to each other while the two oxygen atoms from NQ1 are coordinated *trans* to the two amine nitrogen atoms. For the other two possible configurations, known as *cis*- β (Fig. 3), the two pyridine groups are mutually *cis*, with the hydroxyl and carbonyl oxygen atoms of NQ1 coordinated *trans* to one pyridine and one amine nitrogen atoms, or *vice-versa*. The *cis*- α conformation seems to be favored by relieve of steric strains present in the *cis*- β isomer. For the *cis*- β isomer, the pyridine rings are in a closer proximity, which creates a mutual repulsion that increases the $\text{N}^{\text{py}}\text{-Co-N}^{\text{py}}$ angle to 99° (see Table S2 for selected bond distances and angles). The $\text{N}^2(\text{py})$ also become much closer to the $\text{N}^4\text{H}(\text{en})$ (2.437 Å) when compared with the *cis*- α isomer (2.712 Å). Additionally, a relevant difference was observed for the torsion angle of the ethylenediamine backbone ($\text{Co-N}^4\text{-CC} = 15^\circ$ for *cis*- β and 36° for *cis*- α), which also indicates a higher steric strain in the *cis*- β configuration [56,57]. The *cis*- α conformation was also observed in the X-ray structure of the previously reported complexes $[\text{Co}(\text{bhnq})(\text{py}_2\text{en})]\text{BF}_4 \cdot \text{H}_2\text{O}$ and $[\text{Co}(\text{py}_2\text{en})(\text{Tz})](\text{BF}_4)_2 \cdot 2\text{H}_2\text{O}$ ($\text{Tz} = (\text{E})$ -1-phenyl-1H-1,2,3-triazole-4-carbaldehyde) [27,58]. Calculated Co-L bond distances are of 1.9 Å in average, which is within the range expected for a low spin cobalt(III) ion coordinated to *N,O*-donor ligands [27,28,58–61].

3.4. Cyclic voltammetry

The redox behavior of complexes 1–3 was evaluated by cyclic voltammetry (CV) in acetonitrile (Fig. 4). Electrochemical data are summarized in Table 1. A quasi-reversible process (Ic/Ia) was observed at ($E_{1/2}$) 0.47, -0.43 and -0.48 V vs. Fc/Fc^+ for complexes 1–3, respectively, and assigned to the couple $\text{Co}^{3+}/\text{Co}^{2+}$. The average $\text{Co}^{3+}/\text{Co}^{2+}$ potential (-0.46 V) of complexes 1–3 is shifted cathodically in 0.27 V, when compared with the analogous complex $[\text{Co}(\text{tpa})(\text{NQ-CH}_3)]^{2+}$ ($\text{NQ-CH}_3 = 2$ -hydroxy-3-methyl-1,4-naphthoquinone) ($E_{1/2} = -0.19$ V vs Fc/Fc^+), analyzed under similar conditions [28]. Although a direct comparison between these two systems is difficult, due to the distinct nature of both ancillary and naphthoquinone ligands, it seems that neither the position of the hydroxyl group (5 in NQ1 and 2 in NQ-CH_3), nor the substituents (methyl and *p*-tolylthio in NQ2 and NQ3) has a significant effect on the $\text{Co}^{3+}/\text{Co}^{2+}$ potential. Thus, the nature of the ancillary ligands is most likely responsible for the cathodic shift (0.27 V) in 1–3, as py_2en is a better σ -donor than TPA (two pyridyl and two secondary amines vs three pyridyl and one tertiary amine, respectively) [58]. Additional processes present in the CVs of 1–3 (Table 1) are assigned to successive reductions (IIc, IIIC) and oxidations (IIa, IIIa) of coordinated naphthoquinone ligands (Table 1) [28,53].

3.5. Reactivity assays

Reactions of complexes 1–3 with ascorbic acid (1:10) were performed in DMSO/phosphate buffer solutions (1:10) at pH 7.4, 7.0 and 6.2, in an attempt to mimic reduction in healthy and tumor cells environments. The reactions were carried out from freshly prepared solutions of the complexes and ascorbic acid, and monitored by UV–Vis spectroscopy at room temperature ($25 \pm 2^\circ\text{C}$) under aerobic conditions. An immediate spectral change was observed after addition of

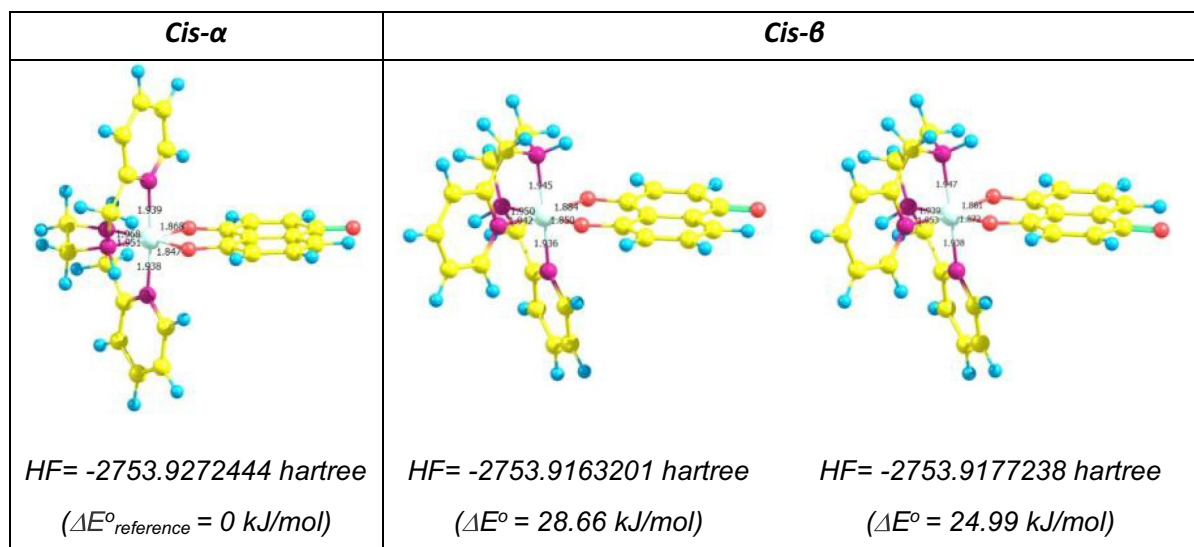


Fig. 3. Evaluation of the geometry and total electronic energy of cis- α and cis- β isomers for $[\text{Co}(\text{NQ1})(\text{py}_2\text{en})]^{2+}$.

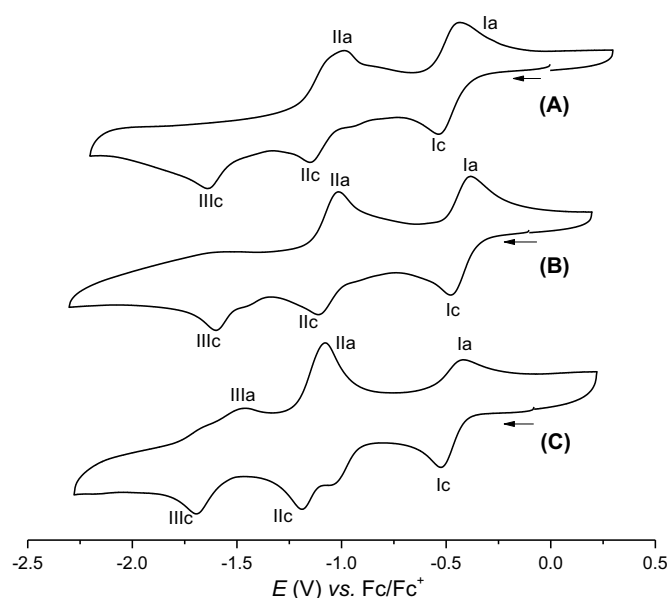


Fig. 4. CVs of 1 (A), 2 (B) and 3 (C) in 0.1 M MeCN/TBAClO₄ at 0.1 V s⁻¹. Ag/AgCl for organic solvent (BASi) was used as reference electrode, and ferrocene was used as internal reference [37].

ascorbic acid to the solutions of the complexes (Fig. 5, S23-S30). The two absorptions (~350 and ~550 nm) present in the spectra of 1–3 disappear, giving rise to a single band in ~420 nm, which is similar in wavelength and intensity to that of the free NQ ligands measured under identical conditions. These results indicate that fast dissociation of the NQ ligands takes place after reduction from Co³⁺ to Co²⁺, with

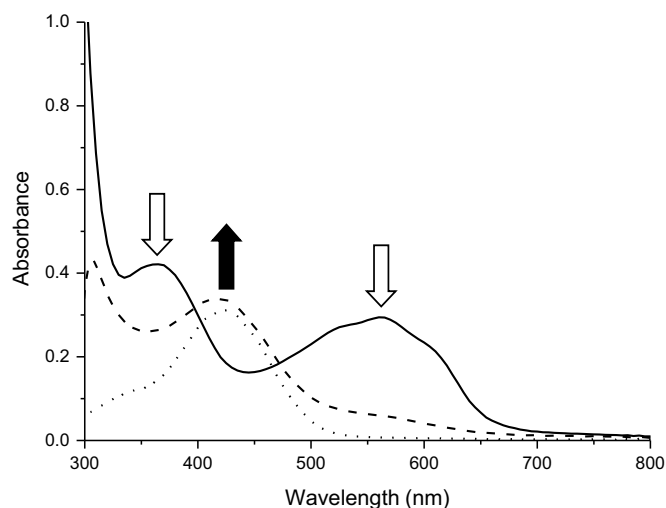


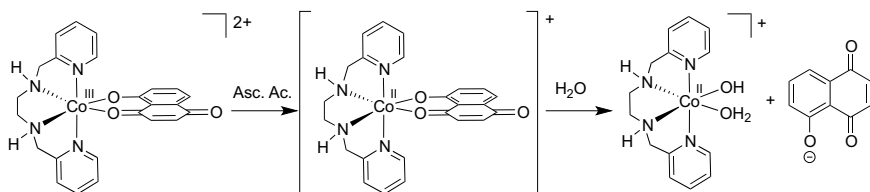
Fig. 5. Spectra of NQ1 and 1 in DMSO/phosphate buffer at pH 6.2 at room temperature, prior and after addition of ascorbic acid (10-fold excess): 1 (— solid line), 1 + AA (— dashed line), NQ1 + AA (... dotted line). Similar spectra were at pH 7.0 and 7.4 for 1 and for complexes 2 and 3 at pH 6.2, 7.0 and 7.4 (Fig. S23–S30).

negligible influence of the pH. To confirm that ligand dissociation only occurs after reduction, control experiments were performed for the complexes in the absence of ascorbic acid. Since no relevant spectral changes were observed during a 1 h period (Fig. S14–S22), spontaneous ligand dissociations induced by the solvent solution within the time scale of the experiment were discarded [62]. Nonetheless, the spectral changes become relevant on a larger time scale (monitored within a

Table 1

CV data (V vs. Fc/Fc⁺) for complexes 1–3, in MeCN.

Complexes	Co ³⁺ /Co ²⁺				NQ/NQ ¹⁻		NQ ¹⁻ /NQ ²⁻	
	Ic	Ia	ΔE	$E_{1/2}$	IIc	IIa	IIIc	IIIa
$[\text{Co}(\text{NQ1})(\text{py}_2\text{en})]^{2+}$ (1)	-0.52	-0.42	0.10	0.47	-1.13	-0.99	-1.63	
$[\text{Co}(\text{NQ2})(\text{py}_2\text{en})]^{2+}$ (2)	-0.48	-0.38	0.10	0.43	-1.10	-1.00	-1.59	
$[\text{Co}(\text{NQ3})(\text{py}_2\text{en})]^{2+}$ (3)	-0.53	-0.43	0.10	0.48	-1.19	-1.08	-1.70	-1.47



Scheme 2. Ligand dissociation upon reduction of complex 1 by ascorbic acid.

72 h interval – data not shown), specially for complex 2, which seems to be more susceptible to ligand exchange by a hydrolytic pathway. These results are comparable to those obtained for the analogous complex $[\text{Co}(\text{tpa})(\text{NQ}-\text{CH}_3)]^{2+}$ [28] and thus indicate that the position of the hydroxyl group, as well as the presence of additional radicals (methyl and *p*-tolylthio) in the NQ ligands, do not have a significant effect on the reactivity of the complexes towards reduction and ligand dissociation (Scheme 2). As the NQ ligands dissociate quickly ($t < 5$ min) upon reduction under aerobic conditions, these complexes are not expected to present hypoxic selectivity in biological conditions.

3.6. Cytotoxic activity

The cytotoxic activity of complexes 1 and 3 was evaluated by MTT assay under conditions of normoxia and hypoxia for 72 h on HCT-116 and HT-29 cell lines. Control experiments were carried out for the free ligands NQ1, NQ3 and py_2en , for cobalt perchlorate and for tirapazamine as a positive reference. The results are showed in Table 2 and the data are presented as mean \pm standard deviation obtained from three independent experiments performed in triplicate. In general, complexes 1 and 3 showed a better activity against HCT-116 cells, while the corresponding free ligands NQ1 and NQ3 performed equally for both cell lines. When compared with its free ligand NQ1, complex 1 was more active for both lineages, while complex 3 was on average four times more active than NQ3 against HCT-116 under both normoxia and hypoxia. Complex 3 also performed approximately three times better than NQ3 against HT-29 and four times better against HT-29 under normoxia. The better activity under normoxia suggest the generation of reactive oxygen species (ROS), which is a well-known mechanism of action of naphthoquinones [29],[63]. Although both complexes 1 and 3 presented better activity than TPZ, none have shown selectivity for hypoxia. The lack of hypoxic selectivity may be explained by the fast dissociation of the NQ ligands observed in the reactivity assays. To be selectively activated in a hypoxic environment, both cobalt(III) and cobalt(II) complexes should resist ligand exchange by the solvent in normoxic conditions, while the cobalt(II) complex must remain stable long enough to be oxidized back by O_2 under normoxia. Nevertheless, the lack of hypoxic selectivity does not prevent cobalt(III) chaperones from improving the activity of a drug in many distinct ways, such as modifying the pharmacokinetic properties and improving cellular uptake [5,6,64].

Table 2

Cytotoxicity of compounds on HCT-116 and HT-29 cells (IC_{50} , μM)^{*}.

Compounds	HCT-116		HT-29	
	Normoxia	Hypoxia	Normoxia	Hypoxia
Complex 1	10.2 \pm 4.0	10.9 \pm 0.2	17.8 \pm 5.3	26.1 \pm 2.1
Complex 3	5.2 \pm 1.5	7.6 \pm 5.1	5.7 \pm 0.2	23.7 \pm 7.0
NQ1	13.3 \pm 1.3	28.8 \pm 4.4	14.2 \pm 2.8	21.9 \pm 8.1
NQ3	20.6 \pm 3.6	36.7 \pm 5.4	22.6 \pm 3.3	34.8 \pm 10.0
py_2en	14.1 \pm 4.1	25.8 \pm 6.6	39.1 \pm 4.3	38.4 \pm 6.6
$\text{Co}(\text{ClO}_4)_2 \cdot 6\text{H}_2\text{O}$	> 100	> 100	> 100	> 100
TPZ	57.6 \pm 24.6	11.1 \pm 0.7	72.6 \pm 0.8	25.5 \pm 9.6

^{*} > 100: at the highest concentration tested (100 μM), inhibition of 50% of cell viability was not achieved and means that the IC_{50} is above that value.

4. Conclusions

The structure, properties and reactivity of three cobalt(III) complexes with 5-hydroxy-1,4-naphthoquinones were investigated for their potential to function as hypoxia activated prodrugs. DFT calculations suggest that the NQ ligands are coordinated in a bidentate mode and the py_2en ancillary ligand occupies the four remaining positions in a *cis- α* configuration. Reactivity studies simulating bioreduction by ascorbic acid revealed a fast and irreversible (O_2 -independent) dissociation of the NQ ligand associated with $\text{Co}^{3+}/\text{Co}^{2+}$ reduction under aerobic conditions, as previously observed for the analogous complex $[\text{Co}(\text{tpa})(\text{NQ}-\text{CH}_3)]^{2+}$ [28]. The lack of hypoxic selectivity was confirmed by *in vitro* cytotoxicity activity assays against HCT-116 and HT-29 cell lines under hypoxic and normoxic conditions. Both complexes 1 and 3 were more active than the reference compound TPZ, with a slightly better performance in normoxia. This result is consistent with the involvement of ROS, which are typically generated by naphthoquinones. Despite the lack of selectivity for hypoxia, a significant improvement in the cytotoxicity of the complexes compared with the naphthoquinones alone was observed and should be investigated further. The absence of hypoxic selectivity is attributed to the redox potential, which facilitates $\text{Co}^{3+}/\text{Co}^{2+}$ reduction but does not allow reoxidation by O_2 , along with low thermodynamic and kinetic stability of the cobalt(II)-NQ complex. In order to achieve selective dissociation of an NQ-based drug under hypoxia upon redox activation, further modifications on the NQ skeleton may be necessary to strengthen its coordination to the metal center. Additionally, the redox potential for the $\text{Co}^{3+}/\text{Co}^{2+}$ has to be adjusted into the ideal range of -0.2 to -0.4 V vs. SHE, by improving the electron-donor capabilities of the ancillary and/or NQ ligands.

CRediT authorship contribution statement

Marcos Vinícius Palmeira de Mello:Methodology, Investigation, Validation, Writing - original draft. **Gerardo Cebrián-Torrejón:**Methodology. **Jonas Ramos Pereira:**Investigation. **Caroline dos Santos Moreira:**Resources. **Carinne Borges de Souza Moraes Rego Gomes:**Resources. **David Rodrigues da Rocha:**Resources. **Elaine Maria de Souza Fagundes:**Methodology, Supervision, Formal analysis, Validation. **Glaucio Braga Ferreira:**Investigation, Validation, Writing - review & editing. **Mauricio Lanznaster:**Conceptualization, Methodology, Supervision, Resources, Project administration, Funding acquisition, Writing - original draft, Writing - review & editing.

Acknowledgements

This work was supported by the Coordenação de Aperfeiçoamento de Pessoal de Nível Superior - Brazil (CAPES) - Finance Code 001 and by the Conselho Nacional de Desenvolvimento Científico e Tecnológico - Brazil (CNPq 406593/2013-2 and 310768/2016-0). M. Lanznaster thanks LAME (Laboratório Multiusuário de Espectroscopia da Universidade Federal Fluminense) and LAMEM (Laboratório Multiusuário de Espectrometria de Massas da Universidade Federal Fluminense) for the use of their facilities.

Appendix A. Supplementary data

Supplementary data to this article can be found online at <https://doi.org/10.1016/j.jinorgbio.2019.110756>.

References

- [1] W.R. Wilson, M.P. Hay, *Nat. Rev. Cancer* 11 (2011) 393–410, <https://doi.org/10.1038/nrc3064>.
- [2] W.A. Denny, *Future Oncol.* 6 (2010) 419–428, <https://doi.org/10.2217/fon.10.11>.
- [3] N. Graf, S.J. Lippard, *Adv. Drug Deliv. Rev.* 64 (2012) 993–1004, <https://doi.org/10.1016/j.addr.2012.01.007>.
- [4] W.R. Wilson, J.W. Moselen, S. Cliffe, W.A. Denny, D.C. Ware, *Int. J. Radiat. Oncol. Biol. Phys.* 29 (1994) 323–327, [https://doi.org/10.1016/0360-3016\(94\)90283-6](https://doi.org/10.1016/0360-3016(94)90283-6).
- [5] M.D. Hall, T.W. Failes, N. Yamamoto, T.W. Hambley, *Dalton Trans.* (2007) 3983–3990, <https://doi.org/10.1039/b707121c>.
- [6] A.K. Renfrew, E.S. O'Neill, T.W. Hambley, E. New, *Coord. Chem. Rev.* 375 (2018) 221–233, <https://doi.org/10.1016/j.ccr.2017.11.027>.
- [7] Y. Chen, L. Hu, *Med. Res. Rev.* 29 (2009) 29–64, <https://doi.org/10.1002/med.20137>.
- [8] A.K. Renfrew, *Metallomics* 6 (2014) 1324–1335, <https://doi.org/10.1039/C4MT00069B>.
- [9] P. Zhang, P.J. Sadler, *Eur. J. Inorg. Chem.* (2017) 1541–1548, <https://doi.org/10.1002/ejic.201600908>.
- [10] C.R. Munteanu, K. Suntharalingam, *Dalton Trans.* 44 (2015) 13796–13808, <https://doi.org/10.1039/c5dt02101d>.
- [11] A.K. Renfrew, N.S. Bryce, T. Hambley, *Chem. Eur. J.* 21 (2015) 15224–15234, <https://doi.org/10.1002/chem.201502702>.
- [12] D.C. Ware, W.R. Wilson, W.A. Denny, C.E.F. Rickard, *J. Chem. Soc. Chem. Commun.* (1991) 1171–1173, <https://doi.org/10.1039/C39910001171>.
- [13] D.C. Ware, B.D. Palmer, W.R. Wilson, W.A. Denny, *J. Med. Chem.* 36 (1993) 1839–1846, <https://doi.org/10.1021/jm00104a008>.
- [14] W.R. Wilson, J.W. Moselen, S. Cliffe, W.A. Denny, D.C. Ware, *Int. J. Rad. Oncol.* 29 (2) (1994) 323–327, [https://doi.org/10.1016/0360-3016\(94\)90283-6](https://doi.org/10.1016/0360-3016(94)90283-6).
- [15] D.C. Ware, P.J. Brothers, G.R. Clark, W.A. Denny, B.D. Palmer, W.R. Wilson, *Dalton Trans.* (2000) 925–932, <https://doi.org/10.1039/a909447d>.
- [16] P.R. Craig, P.J. Brothers, G.R. Clark, W.R. Wilson, W.A. Denny, D.C. Ware, *Dalton Trans.* (2004) 611–618, <https://doi.org/10.1039/b311091e>.
- [17] G. Ahn, D.C. Ware, W.A. Denny, W.R. Wilson, *Rad. Res.* 162 (2004) 315–325, <https://doi.org/10.1667/RR3229>.
- [18] G. Ahn, K.J. Bottling, A.V. Patterson, D.C. Ware, M. Terrel, W.R. Wilson, *Biochem. Pharmacol.* 71 (2006) 1683–1694, <https://doi.org/10.1016/j.bcp.2006.03.007>.
- [19] J.Y. Chang, R.J. Stevenson, G. Lu, P.J. Brothers, G.R. Clark, W.A. Denny, D.C. Ware, *Dalton Trans.* 39 (2010) 11535–11550, <https://doi.org/10.1039/c0dt01142h>.
- [20] T.W. Failes, C. Cullinane, C.I. Diakos, N. Yamamoto, J.G. Lyons, T.W. Hambley, *Chem. Eur. J.* 13 (2007) 2974–2982, <https://doi.org/10.1002/chem.200601137>.
- [21] A.K. Renfrew, N.S. Bryce, T.W. Hambley, *Chem. Sci.* 4 (2013) 3731, <https://doi.org/10.1039/c3sc51530c>.
- [22] A.K. Renfrew, N.S. Bryce, T.W. Hambley, *Chem. Eur. J.* 21 (2015) 15224–15234, <https://doi.org/10.1002/chem.201502702>.
- [23] A. Glenister, C.K.J. Chen, E.M. Tondl, D. Paterson, T.W. Hambley, A.K. Renfrew, *Metallomics* 9 (2017) 699–705, <https://doi.org/10.1039/c6mt00275d>.
- [24] F.L.S. Bustamante, F.S. Miranda, F.A.V. Castro, J.A.L.C. Resende, M.D. Pereira, M. Lanznaster, *J. Inorg. Biochem.* 132 (2014) 37–44, <https://doi.org/10.1016/j.jinorgb.2013.11.007>.
- [25] M.M.P. Silva, L.J. Carvalho, M. Lanznaster, J.A.L.C. Resende, *Acta Cryst. E* E67 (2011) m1489–m1490, <https://doi.org/10.1107/S1600536811038682>.
- [26] F.L.S. Bustamante, M.M.P. Silva, W.A. Alves, C.B. Pinheiro, J.A.L.C. Resende, M. Lanznaster, *Polyhedron* 42 (2012) 43–49, <https://doi.org/10.1016/j.poly.2012.04.027>.
- [27] F.L.S. Bustamante, J.L. Metello, F.A.V. de Castro, C.B. Pinheiro, M.D. Pereira, M. Lanznaster, *Inorg. Chem* 52 (2013) 1167–1169, <https://doi.org/10.1021/ic302175t>.
- [28] A.F.M. da Silva, R.D.U. Vital, D.D.L. Martins, D.R. Rocha, G.B. Ferreira, J.A.L.C. Resende, M. Lanznaster, *New J. Chem.* 41 (2017) 14960–14965, <https://doi.org/10.1039/c7nj03072j>.
- [29] F.C. da Silva, V.F. Ferreira, *Curr. Org. Synth.* 13 (2016) 334–371, <https://doi.org/10.2174/1570179412666150817220343>.
- [30] C. Asche, *Mini-Rev. Med. Chem.* 5 (2005) 449–467, <https://doi.org/10.2174/1389557053765556>.
- [31] B.K. Jha, H. Jung, I. Seo, S. Suh, M. Suh, W. Baek, *Exp. Parasitol.* 159 (2015) 100–106, <https://doi.org/10.1016/j.exppara.2015.09.005>.
- [32] G.H. Hwang, J.M. Ryu, Y.J. Jeon, J. Choi, H.J. Han, Y.M. Lee, S. Lee, J.S. Bae, J.W. Jung, W. Chang, L.K. Kim, J.G. Jee, M.Y. Lee, *J. Eur. J. Pharmacol.* 765 (2015) 384–393, <https://doi.org/10.1016/j.ejphar.2015.08.058>.
- [33] Y.B. Ji, Z.Y. Qu, X. Zou, *Exp. Toxicol. Pathol.* 63 (2011) 69–78, <https://doi.org/10.1016/j.etp.2009.09.010>.
- [34] J. Li, L. Shen, F. Lu, Y. Qin, R. Chen, J. Li, Y. Li, H. Zhan, Y. He, *Acta Pharmacol. Sin.* 33 (2012) 242–249, <https://doi.org/10.1038/aps.2011.152>.
- [35] P. Seshadri, A. Rajaram, R. Rajaram, *Free Radic. Biol. Med.* 51 (2011) 2090–2107, <https://doi.org/10.1016/j.freeradbiomed.2011.09.009>.
- [36] C.-K. Ruy, J.-Y. Shim, M.J. Chae, I.H. Choi, J.-Y. Han, O.-J. Jung, J.Y. Lee, S.H. Jeong, *Eur. J. Med. Chem.* 40 (2005) 438–444, <https://doi.org/10.1016/j.ejmech.2004.12.004>.
- [37] J.O.S. Varejao, L.C.A. Barbosa, C.R.A. Maltha, M.R. Lage, M. Lanznaster, J.W.M. Carneiro, G. Forlani, *Electrochim. Acta* 120 (2014) 334–343, <https://doi.org/10.1016/j.electacta.2013.12.053>.
- [38] R.R. Gagne, C.A. Koval, G.C. Lisensky, *Inorg. Chem.* 19 (1980) 2854–2855, <https://doi.org/10.1021/ic50211a080>.
- [39] D.R. Rocha, V.F. Ferreira, A.C.G. Souza, J.A.L.C. Resende, W.C. Santos, E.A. Santos, C. Pessoa, M.O. Moraes, L.V. Costa-Lotufo, R.C. Montenegro, *Org. Biomol. Chem.* 9 (2011) 4315–4622, <https://doi.org/10.1039/C1OB05209H>.
- [40] M. Lanznaster, A. Neves, I. Vencato, A.J. Bortoluzzi, H. Gallardo, S.P. Machado, A.M.C. Assumpção, *J. Braz. Chem. Soc.* 17 (2) (2006) 289–295, <https://doi.org/10.1590/S0103-50532006000200011>.
- [41] R.N. Firmo, I.C.A. de Souza, F.S. Miranda, C.B. Pinheiro, J.A.L.C. Resende, M. Lanznaster, *Polyhedron* 117 (2016) 604–611, <https://doi.org/10.1016/j.poly.2016.06.022>.
- [42] R.C. Batista, F.S. Miranda, C.B. Pinheiro, M. Lanznaster, *Eur. J. Inorg. Chem.* (2018) 612–616, <https://doi.org/10.1002/ejic.201701251>.
- [43] A.F.M. Silva, M.V.P. Mello, J.G. Gómez, G.B. Ferreira, M. Lanznaster, *Eur. J. Inorg. Chem.* (2018), <https://doi.org/10.1002/ejic.201801550> accepted.
- [44] M.J. Frisch, G.W. Trucks, H.B. Schlegel, G.E. Scuseria, M.A. Robb, J.R. Cheeseman, V.G. Zakrzewski, J.A. Montgomery, R.E. Stratmann, J.C. Burant, S. Dapprich, J.M. Millam, A.D. Daniels, K.N. Kudin, M.C. Strain, O. Farkas, J. Tomasi, V. Barone, M. Cossi, R. Cammi, B. Mennucci, C. Pomelli, C. Adamo, S. Clifford, J. Ochterski, G.A. Petersson, P.Y. Ayala, Q. Cui, K. Morokuma, D.K. Malick, A.D. Rabuck, K. Raghavachari, J.B. Foresman, J. Cioslowski, J.V. Ortiz, A.G. Baboul, B.B. Stefanov, G. Liu, A. Liashenko, P. Piskorz, I. Komaromi, R. Gomperts, R.L. Martin, D.J. Fox, T. Keith, M.A. Al-Laham, C.Y. Peng, A. Nanayakkara, C. Gonzalez, M. Challacombe, P.M.W. Gill, B. Johnson, W. Chen, M.W. Wong, J.L. Andres, C. Gonzalez, M. Head-Gordon, E.S. Replogle, J.A. Pople, GAUSSIAN 09 (Revision D. 01), Gaussian Inc., Pittsburgh, PA, 2009.
- [45] Chemcraft, <http://www.chemcraftprog.com> (accessed September 2018).
- [46] C. Adamo, V. Barone, *J. Chem. Phys.* 110 (1999) 6158–6169, <https://doi.org/10.1063/1.478522>.
- [47] T. Mosmann, *J. Immunol. Methods* 65 (1983) 55–63, [https://doi.org/10.1016/0022-1759\(83\)90303-4](https://doi.org/10.1016/0022-1759(83)90303-4).
- [48] L.R. Harrison, D. Micha, M. Brandenburg, K.L. Simpson, C.J. Morrow, O. Denny, C. Hodgkinson, Z. Yunus, C. Dempsey, D. Roberts, F. Blackhall, G. Makin, C. Dive, *J. Clin. Invest.* 121 (2011) 1075–1087, <https://doi.org/10.1172/JCI43505>.
- [49] N.E. Dixon, W.G. Jackson, M.J. Lancaster, G.A. Lawrance, A.M. Sargeson, *Inorg. Chem.* 20 (1981) 470–476, <https://doi.org/10.1021/ic50216a031>.
- [50] F.L.S. Bustamante, M.M.P. Silva, W.A. Alves, C.B. Pinheiro, J.A.L.C. Resende, M. Lanznaster, *Polyhedron* 42 (2012) 43–49, <https://doi.org/10.1016/j.poly.2012.04.027>.
- [51] M.A. Ribeiro, M. Lanznaster, M.M.P. Silva, J.A.L.C. Resende, M.V.B. Pinheiro, K. Krambrock, H.O. Stumpf, C.B. Pinheiro, *Dalton Trans.* 42 (2013) 5462–5470, <https://doi.org/10.1039/c3dt32968b>.
- [52] A.I. Francisco, M.D. Vargas, J.W.M. Carneiro, M. Lanznaster, J.C. Torres, C.A. Camara, A.C. Pinto, *J. Mol. Structure* 891 (2008) 228–232, <https://doi.org/10.1016/j.molstruc.2008.03.028>.
- [53] A.F.M. Silva, C.B. Pinheiro, J.A.L.C. Resende, M. Lanznaster, *Polyhedron* 123 (2017) 132–137, <https://doi.org/10.1016/j.poly.2016.10.042>.
- [54] K. Nakamoto, *Infrared and Raman Spectra of Inorganic and Coordination Compounds*, 4rd ed., John Wiley, New York, 1986, p. 253.
- [55] A.M. Sargeson, G.H. Searle, *Inorg. Chem.* 6 (1967) 787–796, <https://doi.org/10.1021/ic50050a029>.
- [56] J.G. Gibson, E.D. McKenzie, *J. Chem. Soc. A* (1971) 1666–1683, <https://doi.org/10.1039/J19710001666>.
- [57] K. Dyduch, M. Srebro-Hooper, B.Y. Lee, A. Michalak, *J. Comput. Chem.* 39 (2018) 1854–1867, <https://doi.org/10.1002/jcc.25358>.
- [58] I.C.A. de Souza, L.V. Faro, C.B. Pinheiro, D.T.G. Gonzaga, F.C. Silva, V.F. Ferreira, F.S. Miranda, M. Scarpellini, M. Lanznaster, *Dalton Trans.* 45 (2016) 13671–13674, <https://doi.org/10.1039/C6DT02456D>.
- [59] B.M. Pires, L.C. Giacomini, F.A.V. Castro, A.S. Cavalcanti, M.D. Pereira, A.J. Bortoluzzi, R.B. Faria, M. Scarpellini, *J. Inorg. Biochem.* 157 (2016) 104–113, <https://doi.org/10.1016/j.jinorgbio.2016.01.024>.
- [60] E.T. Souza, L.C. Castro, F.A.V. Castro, L.C. Visentin, C.B. Pinheiro, M.C. Pereira, S.P. Machado, M. Scarpellini, *J. Inorg. Biochem.* 103 (2009) 1355–1365, <https://doi.org/10.1016/j.jinorgbio.2009.07.008>.
- [61] E.T. Souza, P.J.S. Maia, E.M. Azevedo, C.R. Kaiser, J.A.L.C. Resende, C.B. Pinheiro, T.A. Heinrich, R.S. Silva, M. Scarpellini, *J. Inorg. Biochem.* 12 (2011) 1767–1773, <https://doi.org/10.1016/j.jinorgbio.2011.09.011>.
- [62] For more details see Figures S14–S22 in the ESI file.
- [63] Y.G. de Paiva, F. da R. Ferreira, T.L. Silva, E. Labbé, O. Buriez, C. Amatore, M.O.F. Goulart, *Curr. Top. Med. Chem.* 15 (2015) 136–162, <https://doi.org/10.2174/1568026615666141209155300>.
- [64] M.C. Heffern, N. Yamamoto, R.J. Holbrook, A.L. Eckermann, T.J. Meade, *Curr. Opin. Chem. Biol.* 17 (2013) 189–196, <https://doi.org/10.1016/j.cbpa.2012.11.019>.